Flat bands with Berry curvature in multilayer graphene

Akshay Kumar and Rahul Nandkishore

Flat bands with local Berry curvature in multilayer graphene

Akshay Kumar[1] and Rahul Nandkishore[2, *]

[1]*Department of Physics, Princeton University, Princeton, NJ 08544, USA*
[2]*Princeton Center for Theoretical Science, Princeton University, Princeton, NJ 08544, USA*

We demonstrate that flat bands with local Berry curvature arise naturally in chiral (ABC) multilayer graphene placed on a boron nitride (BN) substrate. The degree of flatness can be tuned by varying the number of graphene layers N. For $N = 7$ the bands become nearly flat, with a small bandwidth ~ 3.6 meV. The two nearly flat bands coming from the K and K' valleys cross along lines in the reduced zone. Weak intervalley tunneling turns the bandcrossing into an avoided crossing, producing two nearly flat bands with global Chern number zero, but with local Berry curvature. The flatness of the bands suggests that many body effects will dominate the physics, while the local Berry curvature of the bands endows the system with a nontrivial quantum geometry. The quantum geometry effects manifest themselves through the quantum distance (Fubini-Study) metric, rather than the more conventional Chern number. Multilayer graphene on BN thus provides a platform for investigating the effect of interactions in a system with a non-trivial quantum distance metric, without the complication of non-zero Chern numbers. We note in passing that flat bands with non-zero Chern number can also be realized by making use of magnetic adatoms, and explicitly breaking time reversal symmetry.

The behavior of strongly interacting electrons and the effect of quantum geometry are two of the most exciting fields of research in modern condensed matter physics. Strong interactions can give rise to effects such as fractionalization [1–3], where the elementary excitations carry some fraction of the 'fundamental' electronic quantum numbers. One popular way to access strong correlation physics is to consider band structures that are flat (non-dispersive), since in such band structures interactions naturally dominate over kinetic energy. Meanwhile, the two ingredients of quantum geometry are integrated Berry curvature (a.k.a. Chern number for two dimensional systems) and Fubini-Study metric [4], the metric measuring the quantum distance. While non-zero integrated Berry curvature can lead to the existence of states that are protected against disorder [5–7] and to effects like quantized Hall conductance of a band insulator [8], non-zero Fubini Study metric can lead to phenomena such as pseudospin conservation laws in single layer graphene [4] and unusual features in the current noise spectrum of a band insulator [9]. Recently, a strong interest has emerged in flat band systems as playgrounds for investigating the interplay of strong correlation effects and non-trivial quantum geometry. However, attention has been mostly focused on systems with non-zero integrated Berry curvature, [11–20], while the effect of the Fubini-Study metric has largely been ignored.

The influence of quantum geometry on the strong correlation physics stems from the fact that the interactions couple to electron density, and the electron density operators projected onto the flat band obey a non-trivial commutation relation if the band has a non-trivial quantum geometry [16,21]. The general commutation relation for projected densities in a band with non-uniform Berry curvature is [21]:

$$[\bar{\rho}_{\mathbf{q1}}, \bar{\rho}_{\mathbf{q2}}] \approx i\mathbf{q1} \wedge \mathbf{q2} \sum_{\mathbf{k},b} [B(\mathbf{k})u_b^*(\mathbf{k}_+)u_b(\mathbf{k}_-)\gamma_{\mathbf{k}_+}^\dagger \gamma_{\mathbf{k}_-}] \quad (1)$$

where $\mathbf{q1} \wedge \mathbf{q2} = \hat{z}.(\mathbf{q_1} \times \mathbf{q_2})$, $\mathbf{k}_\pm = \mathbf{k} \pm \frac{\mathbf{q_1}+\mathbf{q_2}}{2}$, $B(\mathbf{k})$ is the local Berry curvature for the band of interest for the single-particle hamiltonian $H = \sum_{\mathbf{k},a,b} c_{\mathbf{k},a}^\dagger h_{ab}(\mathbf{k})c_{\mathbf{k},b}$ and the corresponding eigenstate is given by $|\mathbf{k}\rangle = \gamma_{\mathbf{k}}^\dagger |0\rangle = \sum_a u_a(\mathbf{k})c_{\mathbf{k},a}^\dagger |0\rangle$. Thus far, attention has been focused on systems where the Berry curvature is nearly uniform [11–20]. However, it is apparent from (1) that non-trivial quantum geometry effects do not require a uniform Berry curvature. The influence of the quantum distance metric may be most clearly revealed in a flat band system with local Berry curvature, but zero integrated Berry curvature, since here the non-trivial quantum geometry effects (encoded e.g. in the projected density commutator) arise purely due to the metric. Thus far, theoretical studies have largely ignored this exciting direction of research, in part because of the lack of experimental realizations.

In this article, we show that flat bands with local Berry curvature (but vanishing integrated Berry curvature) arise naturally in chiral multilayer graphene. Our proposal exploits the fact that ABC stacked multilayer graphene in the presence of a perpendicular electric field has a bandstructure with flat pockets that possess Berry curvature. Placing the graphene on a hexagonal Boron Nitride (BN) substrate then produces a superlattice potential such that the reduced Brillouin zone lies entirely within the flat pocket. Umklapp scattering opens a bandgap at the reduced zone edge. For a N layer system with $N > 5$ layers, the lowest band is nearly flat, with a bandwidth $\sim 5meV$. We have verified that this nearly flat band has a non-vanishing local Berry curvature. Chiral multilayer graphene thus provides an ideal platform for investigating the interplay of strong correlations and quantum geometry, with the quantum geometry effects coming from the (hitherto neglected) channel of the Fubuni-Study metric, rather than the more conventional channel of non-zero Chern number. As such, we believe chiral multilayer graphene offers an exciting

new frontier in the study of systems with an interplay of strong correlations and quantum geometry.

We note in passing that a non-zero integrated Berry curvature can also be obtained by using magnetic adatoms rather than vertical electric field to open a gap between conduction and valence bands.

ABC stacked graphene: A single graphene sheet consists of a honeycomb lattice of carbon atoms. The honeycomb lattice consists of two sublattices, A and B. Chiral multilayer graphene consists of graphene sheets with an ABC stacking order (each succeeding sheet is rotated by $2\pi/3$ relative to the preceding sheet). Every lattice site in the bulk is either directly above or directly below another lattice site. In the $(\psi_{1A\mathbf{k}}\psi_{1B\mathbf{k}}\psi_{2A\mathbf{k}}\psi_{2B\mathbf{k}}\cdots\cdots\psi_{NA\mathbf{k}}\psi_{NB\mathbf{k}})$ basis, the nearest neighbor tight binding Hamiltonian for an N layer system takes the form [22]

$$H_0 = \begin{pmatrix} 0 & t_{\mathbf{p}} & 0 & 0 & 0 & 0 & \cdots \\ t_{\mathbf{p}}^* & 0 & \gamma & 0 & 0 & 0 & \cdots \\ 0 & \gamma & 0 & t_{\mathbf{p}} & 0 & 0 & \cdots \\ 0 & 0 & t_{\mathbf{p}}^* & 0 & \gamma & 0 & \cdots \\ 0 & 0 & 0 & \gamma & 0 & t_{\mathbf{p}} & \cdots \\ 0 & 0 & 0 & 0 & t_{\mathbf{p}}^* & 0 & \cdots \\ \vdots & \vdots & \vdots & \vdots & \vdots & \vdots & \ddots \end{pmatrix} \quad (2)$$

Here, $t_{\mathbf{p}} = t_0\big(\exp(ik_x a) + 2\exp(-i\frac{k_x a}{2})\cos(\frac{\sqrt{3}k_y a}{2})\big)$, represents nearest neighbor hopping within each graphene layer ($t_0 \approx 3eV$), and $\gamma \approx 300 meV$ represents interlayer hopping between two sites that lie on top of each other. Here a is the lattice constant of graphene.

In the absence of interlayer hopping, $\gamma = 0$, the bandstructure consists of N copies of the graphene bandstructure, $E = \pm|t_{\mathbf{p}}|$ [25]. Near the two inequivalent corners of the Brillouin zone, conventionally labelled K and K', the function $t_{\mathbf{p}}$ vanishes as $t_{\mathbf{p}} \approx v\mathbf{p}_+$ and $t_{\mathbf{p}} \approx -v\mathbf{p}_-$ respectively, where $\mathbf{p}_\pm = p_x \pm ip_y$ and $v = 3at_o/2$ is the Fermi velocity for graphene.

We now consider interlayer hopping $\gamma \neq 0$. This interlayer hopping causes all the bulk sites to dimerize, opening up a bulk gap of size γ at the Dirac points. On the top and bottom surfaces, there are undimerized lattice sites, which give rise to gapless surface states. The low energy single particle Hamiltonian for the surface states of an N layer graphene takes the form [23,24,26,27,30]

$$H_K(\mathbf{p}) = \frac{v^N}{(-\gamma)^{N-1}} \begin{pmatrix} 0 & p_+^N \\ p_-^N & 0 \end{pmatrix}; \quad p_\pm = p_x \pm ip_y \quad (3)$$

Here H_K is the Hamiltonian in the K valley, and the Hamiltonian in the K' valley is given by $H_{K'}(\mathbf{p}) = H_K^*(-\mathbf{p})$. The basis is such that $(1,0)$ is a Bloch state in the A sublattice of the top layer, and $(0,1)$ is a Bloch state in the B sublattice of the bottom layer. Only the lowest order terms have been written in each matrix element. This Hamiltonian is valid up to an energy scale γ. Note that this energy scale is independent of N, the number of layers of graphene. The above effective Hamiltonian consists of a single bandcrossing with
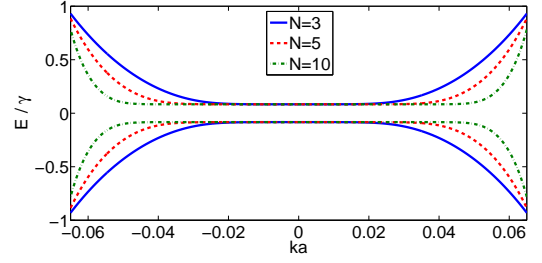

FIG. 1: Low energy band structure for N layer ABC stacked graphene in the presence of a vertical electric field. The band structure is plotted in the vicinity of the $\mathbf{K}$ point, assuming that the potential difference between the top and bottom layers $\Delta = 0.167t_0 \approx 50meV$.

non-trivial Berry phase $N\pi$, and low energy dispersion $E = \pm v^N p^N/\gamma^{N-1}$. Thus, the conduction band has a very flat pocket of a size $p \sim \gamma/v$ around the K and K' points, and this pocket becomes perfectly flat in the limit $N \to \infty$, corresponding to 'rhombohedral graphite'. The emergence of this flat pocket has previously been discussed in [23,24].

Now consider the application of a vertical electric field leading to potential difference V between any 2 consecutive layers. We assume that $\gamma \gg e(N-1)V$. This ensures that the surface bands are much below the bulk bands. The low energy effective Hamiltonian then takes the form

$$H_K(\mathbf{p}) = \begin{pmatrix} \frac{\Delta}{2} & \frac{v^N}{(-\gamma)^{N-1}}p_+^N \\ \frac{v^N}{(-\gamma)^{N-1}}p_-^N & -\frac{\Delta}{2} \end{pmatrix} \quad (4)$$

The resulting band structure is plotted in Fig.1. We can see that a gap of magnitude $\Delta = (N-1)eV$ opens in the surface state spectrum. We can also see that the band near the K point is extremely flat, asymptoting to perfect flatness in the limit $N \to \infty$.

Effect of BN substrate: BN is a popular substrate for graphene. It has the same hexagonal structure, but with a slight lattice-mismatch (lattice constant $\sim \frac{56}{55}a$) and is a large band-gap insulator ($E_{gap} \sim 5eV$). Placing multilayer graphene on BN substrate introduces a superlattice potential with a $Z \times Z$ supercell, where $Z = 56$. The primitive lattice vectors corresponding to the reciprocal lattice are

$$\begin{pmatrix} \mathbf{B_1} \\ \mathbf{B_2} \end{pmatrix} = \frac{2\pi}{3Za} \begin{pmatrix} 1 & \sqrt{3} \\ 1 & -\sqrt{3} \end{pmatrix} \begin{pmatrix} \hat{\mathbf{x}} \\ \hat{\mathbf{y}} \end{pmatrix} \quad (5)$$

The strong superlattice potential is seen primarily by states on the lower surface of the multilayer graphene, close to the substrate. These states are either conduction band or valence band states, depending on the sign of the vertical electric field. We assume the electric field is chosen such that it is the conduction band that mainly sees the superlattice potential. If the multilayer graphene were sandwiched between BN sheets, then both conduc-
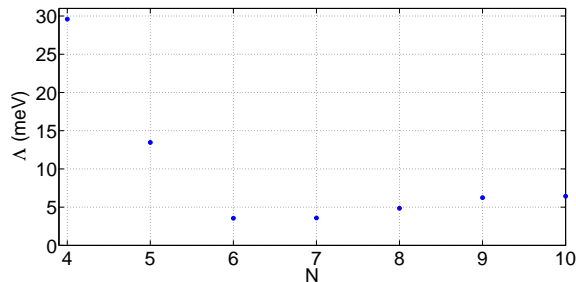
FIG. 2: Bandwidth Λ of the lowest conduction band for N layer chiral graphene. For $N > 5$, the bandwidth comes mainly from umklapp scattering at the zone boundary.

FIG. 3: Dispersions of the three lowest conduction bands for $N = 7$ along the high symmetry directions.

tion and valence bands would see a strong superlattice potential, irrespective of the sign of electric field.

The reduced 'Brillouin zone' for the superlattice is hexagonal, but scaled by a factor $1/Z$ with respect to the original Brillouin zone. If Z is chosen such that $|\mathbf{K}|/Z < \gamma/v$, i.e. $Z > Z_c$, where

$$Z_c = 20\pi/\sqrt{3} = 36.3 \quad (6)$$

then the 'flat pockets' at K and K' extend over the entire reduced Brillouin zone. Moreover, umklapp scattering at the boundaries of the reduced Brillouin zone opens a gap between the flat pocket and the rest of the band. Since for BN substrate, $Z = 56 > Z_c$, it follows that placing chiral multilayer graphene on BN leads to flat bands that extend over the entire reduced Brillouin zone, and which are separated from the rest of the bandstructure by the umklapp energy scale λ.

We now explicitly calculate the bandstructure in the reduced zone. It may be readily determined that for the above superlattice potential, the K and K' points in the original zone get folded to inequivalent corners $\tilde{K}$ and $\tilde{K}'$ of the reduced zone. Meanwhile, the reciprocal lattice vectors of the superlattice satisfy $|\mathbf{B}_{1,2}| < \gamma/v < 2|\mathbf{B}_{1,2}|$, where γ/v is the width of the flat pocket. Since Bragg scattering is only effective between states that are near degenerate, we restrict our attention to Bragg scattering by a single reciprocal lattice vector, and neglect higher order Bragg scattering events. The matrix elements of the superlattice potential $\langle \mathbf{k}|\hat{V}|\mathbf{k} + \mathbf{B}_{1,2}\rangle$ were determined by modelling the BN superlattice as a positive δ-function potential at each B site and a negative δ-function potential at each N site [30]. Hence we obtained the bandstructure in the reduced zone. Although the bandstructure contains $Z^2 = 56^2 = 3136$ conduction bands per spin and valley, only the lowest conduction band is flat, and is separated from the higher bands by an energy scale of order λ, where the gap may be estimated from the DFT calculations in [28], and is of order $10meV$. Meanwhile, the bandgap Δ between conduction and valence bands can be externally controlled using gates, and may be made as large as desired. We should take $\Delta \gg 10meV$ to ensure that we do not mix conduction and valence bands.
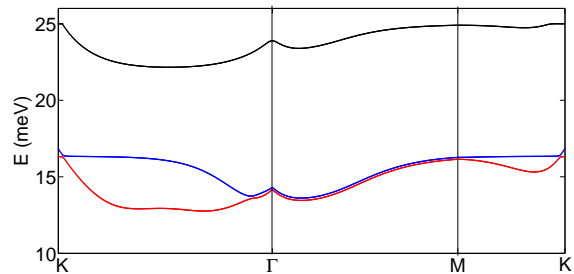
For specificity, we suggest using $\Delta = 50meV$, which is easily achievable by gating [29].

The superlattice potential from the BN substrate also introduces intervalley tunneling of magnitude λ/Z [30], which turns the bandcrossings of the two nearly flat bands coming from K and K' valleys into avoided crossings. The resulting bandstructure contains two strictly non-degenerate flat conduction bands, separated by a minigap $\lambda/Z \approx 0.2meV$. The lowest energy band comes mostly from the K valley in regions closest to the $\tilde{K}$ corner of the reduced zone, and comes mostly from the K' valley in regions closest to the $\tilde{K}'$ corner. From the bandstructure calculations, we can extract the bandwidth of the two low-lying conduction bands. In Fig.2, we plot the bandwidth of the lowest conduction band as a function of N. We see that for $N > 5$ the two low-lying conduction bands are nearly flat, with a small residual bandwidth around 5 meV which comes mainly from umklapp scattering at the zone boundary. The $N = 7$ layer system actually has minimum bandwidth of ~ 3.6 meV, due to a cancellation between 'intrinsic' curvature of the band and the effect of umklapp scattering.

We also note that there is an indirect band gap separating the two flat bands from the higher energy non-flat bands (Fig.3). It vanishes for $N < 6$ and then decreases with increasing N. Transitions across the indirect bandgap must be phonon assisted and should be weak, but nevertheless it is essential that we work with $N > 5$ to have a truly isolated flat band. Fortunately, $N = 7$ is optimal not only through having the flattest band (Fig.2), but also because its indirect band gap is of order the direct band gap. For $N = 7$ the direct band gap is $\sim 6meV$.

We have now verified that the lowest conduction band can be made flat. Now we show that this band has non-vanishing Berry curvature. The momentum-space Berry curvature for the nth band is given by [8]

$$B_n(\mathbf{k}) = -\sum_{n' \neq n} \frac{2Im \langle n\mathbf{k}|v_x|n'\mathbf{k}\rangle \langle n'\mathbf{k}|v_y|n\mathbf{k}\rangle}{(E_{n'} - E_n)^2} \quad (7)$$

where $v_{x(y)}$ is the velocity operator and E_n is the eigenenergy corresponding to the $|n\mathbf{k}\rangle$ eigenstate. It may be readily determined that the K and K' bands have opposite signs of local Berry curvature. The conduction and
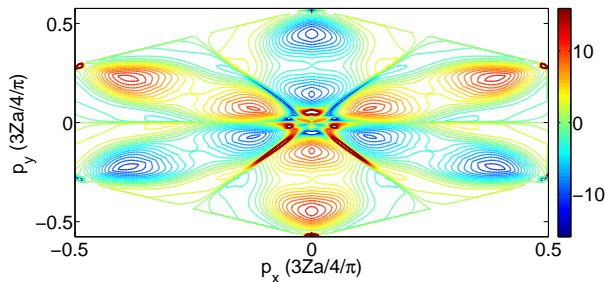
FIG. 4: Contour plot of Berry curvature in the lowest flat conduction band for $N = 7$. The red/yellow regions come mainly from the K valley and have positive curvature, while the blue regions come mainly from the K' valley and have negative curvature. The Berry curvature integrated over the band is zero.

valence bands also have opposite signs of local Berry curvature at every point in momentum space. As a result, when the chemical potential is placed between conduction and valence bands, the system displays quantum valley Hall effect [31]. However, flat band physics will manifest itself when the chemical potential is placed inside either the conduction or the valence bands. In this case we can focus on the band that contains the chemical potential.

We consider the conduction band for specificity. Due to avoided crossings between bands coming from the two valleys, the lowest conduction band contains regions with positive and negative local Berry curvature respectively while the integrated Berry curvature (Chern number) is zero (Fig.4). Meanwhile, there is a second nearly flat conduction band which is separated by a mini gap equal to the inter valley scattering amplitude.

Thus, we conclude that placing $N = 7$ layer ABC graphene on BN substrate allows us to realize two nearly flat bands with local Berry curvature but zero Chern number which are separated from the non-flat bands by a band gap of $6 meV$ and are separated from each other by a minigap of $0.2 meV$, equal to the inter valley scattering amplitude. Chiral multilayer graphene thus offers a promising playground for investigating the effect of strong interactions in the presence of a non-trivial quantum distance metric.

Chern number from adatoms. The key feature of chiral multilayer graphene is that it allows access to a system with a non-trivial quantum geometry but without Chern number. However, a non-zero Chern number may also be obtained by making use of adatom deposition on the outermost graphene layers to open up a gap between conduction and valence bands, rather than using vertical electric field. Adatom deposition also introduces a superlattice potential. For the appropriate choice of (time reversal symmetry breaking) adatoms, the two valleys acquire the same sign of Berry curvature [33–35]. The rest of the analysis proceeds exactly as before, only now the Berry curvature has the same sign everywhere in the flat band, and thus does not cancel.

Concluding remarks. We have shown that ABC stacked multilayer graphene placed on BN substrate has a bandstructure containing flat bands. The seven layer system is ideal for this purpose. The flat bands have nonzero local Berry curvature but zero Chern number. Thus, chiral multilayer graphene represents an exciting new frontier in the study of interaction effects in systems with non-trivial quantum geometry, allowing access to an interaction dominated system with a non-trivial quantum distance metric but without the complication of a non-zero Chern number.

[*] Electronic address: rahuln@princeton.edu

[1] R. Rajaraman, arXiv:cond-mat/0103366 (unpublished).

[2] R.B.Laughlin, Rev. Mod. Phys. 71, 863

[3] J. Martin *et al*, Science 305 (5686): 9803 (2004)

[4] F.D.M. Haldane, Talk at PCCM summer school 2012, `http://wwwphy.princeton.edu/~haldane/talks/pccmsummerschool2012_haldane.pdf`

[5] F.D.M.Haldane, Phys. Rev. Lett. 107, 116801 (2011)

[6] B. Blok and Xiao-Gang Wen. Nucl. Phys. B, 374:615 (1992).

[7] M.Z.Hasan and C.L.Kane, Rev. Mod. Phys. 82, 3045

[8] D. Thouless, M. Kohomoto, M. Nightingale, M. den Nijs, Phys. Rev. Lett. 49,405, (1982)

[9] Titus Neupert, Claudio Chamon, and Christopher Mudry, arXiv:1303.4643

[10] S.M.Girvin and A.H.MacDonald, in S.DasSarma and A.Pinczuk (Eds), *Perspectives in Quantum Hall Effects*, Wiley (1997).

[11] E.Tang, J.-W. Mei and X.G.Wen, Phys. Rev. Lett. 106, 236802 (2011)

[12] T. Neupert, L. Santos, C. Chamon and C. Mudry, Phys. Rev. Lett. 106, 236804 (2011)

[13] K. Sun, Z.-C. Gu, H. Katsura and S. Das Sarma, Phys. Rev. Lett. 106, 236803 (2011)

[14] N. Regnault and B. Andrei Bernevig, Phys. Rev. X 1, 021014 (2011)

[15] Y.-L. Wu, B. A. Bernevig and N. Regnault, Phys. Rev. B 85, 075116 (2012)

[16] S.A.Parameswaran, R. Roy and S. L. Sondhi, Phys. Rev. B 85, 241308(R) (2012)

[17] G. Murthy and R. Shankar, http://arxiv.org/abs/1108.5501

[18] Y.-M.Lu and Y. Ran, Phys. Rev. B 85, 165134 (2012)

[19] M. Trescher and E.J.Bergholtz, http://arxiv.org/abs/1205.2245

[20] C.H.Lee, R. Thomale and X.-L. Qi, http://arxiv.org/abs/1207.5587

[21] Rahul Roy, arXiv:1208.2055

[22] F. Zhang, J. Jung, G.A.Fiete, Q. Niu and A.H.MacDonald, Phys. Rev. Lett. 106, 156801 (2011)

[23] T. T. Heikkila and G.E. Volovik, Pisma Zh.Eksp.Teor.Fiz. 93, 63-68 (2011); JETP Lett. 93, 59-65, (2011)

[24] T.T. Heikkila, N.B. Kopnin, G.E. Volovik, Pis'ma ZhETF 94, 252-258 (2011), (arXiv: 1012.0905)

[25] P.R.Wallace, Phys. Rev. 71, 622634 (1947)

[26] M. Koshino and E. McCann, Phys. Rev. B. 80, 165409 (2009)

[27] M. Nakamura and L. Hirasawa, Phys. Rev. B. 77, 045429 (2008)

[28] B. Sachs, T.O.Wehling, M.I.Katsnelson and A.I. Lichtenstein, Phys. Rev. B 84, 195414 (2011)

[29] Y. Zhang *et al*, Nature, 459, 820-823 (Jun 2009)

[30] See supplementary material.

[31] R. Nandkishore and L. Levitov, Phys. Rev. B, 82, 115124 (2010)

[32] Y.-L.Wu, N. Regnault and B. A. Bernevig, Phys. Rev. B 86, 085129 (2012)

[33] Z. Qiao *et al*, Phys. Rev. B 82, 161414(R) (2010)

[34] H. Zhang, C. Lazo, S. Blugel, S. Heinze and Y. Mokrousov, Phys. Rev. Lett. 108, 056802 (2012)

[35] J. Ding, Z. Qiao, W. Feng, Y. Yao and Q. Niu, Phys. Rev. B 84, 195444 (2011)